EJO
ISSN 1120-6721

Eur J Ophthalmol 2017; 27 (2): 129-134
DOI: 10.5301/ejo.5000850

ORIGINAL RESEARCH ARTICLE

Combined tomography and epithelial thickness mapping for diagnosis of keratoconus

Ronald H. Silverman[1,2], Raksha Urs[1], Arindam RoyChoudhury[3], Timothy J. Archer[4], Marine Gobbe[4], Dan Z. Reinstein[1,4,5]

[1] Department of Ophthalmology, Columbia University Medical Center, New York, NY - USA
[2] F.L. Lizzi Center for Biomedical Engineering, Riverside Research, New York, NY - USA
[3] Department of Biostatistics, Columbia University Medical Center, New York, NY - USA
[4] London Vision Clinic, London - UK
[5] Centre Hospitalier National d'Ophtalmologie des Quinze-Vingts, Paris - France

ABSTRACT

Purpose: Scanning Scheimpflug provides information regarding corneal thickness and 2-surface topography while arc-scanned high-frequency ultrasound allows depiction of the epithelial and stromal thickness distributions. Both techniques are useful in detection of keratoconus. Our aim was to develop and test a keratoconus classifier combining information from both methods.

Methods: We scanned 111 normal and 30 clinical keratoconus subjects with Artemis-1 and Pentacam data. After selecting one random eye per subject, we performed stepwise linear discriminant analysis on a dataset combining parameters generated by each method to obtain classification models based on each technique alone and in combination.

Results: Discriminant analysis resulted in a 4-variable model (R^2 = 0.740) based on Artemis data alone and a 4-variable model (R^2 = 0.734) using Pentacam data alone. The combined model (R^2 = 0.828) consisted of 3 Artemis- and 4 Pentacam-derived variables. The combined model R value was significantly higher than either model alone (p = 0.031, one-tailed). In cross-validation, Artemis had 100% sensitivity and 99.2% specificity, Pentacam had 97.3% sensitivity and 98.0% specificity, and the combined model had 97.3% sensitivity and 100% specificity.

Conclusions: Pentacam, Artemis, and combined models were all effective in distinguishing normal from clinical keratoconus subjects. From the standpoint of variance explained by the model (R^2 values), the combined model was most effective. Application of the model to early and subclinical keratoconus will ultimately be required to assess the effectiveness of the combined approach.

Keywords: Computer-assisted diagnosis, Corneal epithelium, Keratoconus, Tomography, Topography

Introduction

Keratoconus (KC) is a progressive corneal dystrophy characterized by corneal thinning and bulging. Despite the usefulness of topographic and tomographic methods for KC screening, there remain equivocal cases where a confident diagnosis cannot be made. Supplementation of the information provided by these methods by independent quantitative parameters could potentially improve sensitivity and specificity. One such parameter is the thickness distribution of the corneal epithelium. Reinstein et al (1) described how the epithelial thickness profile, derived from high-frequency ultrasound scans, remodels in response to underlying stromal irregularities, and suggested that epithelial remodeling may mask stromal surface changes from anterior surface topography in early KC (2). Using the Artemis (ArcScan Inc., Golden, CO, USA) very-high-frequency ultrasound system, Reinstein et al (3) reported KC corneas to have a donut epithelial thickness pattern characterized by compensatory thinning over the stromal surface cone with a surrounding annulus of thicker epithelium. Silverman et al (4) developed a multivariate classifier for separation of normal and KC eyes based on Artemis-derived epithelial and stromal thickness patterns that allowed full separation of normal from clinical KC. Recent optical coherence tomography–based studies have described similar epithelial thickness patterns in KC corneas (5-7).

In this report, we investigate the merging of epithelial and stromal thickness maps derived from the Artemis with topographic and tomographic data and KC indices derived from Pentacam (Oculus, Wetzlar, Germany) scanning Scheimpflug to assess the effectiveness of each method individually and in combination as a means for differentiating normal and clinical KC corneas. This report is the first to describe this algorithm in

Accepted: July 8, 2016
Published online: August 8, 2016

Corresponding author:
Ronald H. Silverman, PhD
Department of Ophthalmology
Columbia University Medical Center
635 West 165th St., Box #42
10032 New York, NY, USA
rs3072@cumc.columbia.edu

detail. Application of this method to a population of suspect KC eyes will be the subject of a future study.

Methods

This study was conducted under protocols approved by Western Institutional Review Board (Puyallup, WA, USA) and the Institutional Review Board of the Columbia University Medical Center (New York, NY, USA).

In this study, we restricted the subject cohort to unambiguously normal and clinical KC subjects and used stepwise multivariate analysis followed by receiver operating characteristic (ROC) analysis. We randomly selected and analyzed 1 eye from 111 normal and 30 KC subjects from a population of patients seeking refractive surgery at the London Vision Clinic. All subjects were scanned with Artemis-1 and Pentacam.

Assessment of all patients included manifest refraction, logMAR corrected distance visual acuity (CDVA) (CSV-1000; Vector Vision Inc., Greenville, OH, USA), and cycloplegic refraction using one drop of tropicamide 1% (Alcon Laboratories UK Ltd., Hemel Hempstead, UK). Tomography was assessed by Pentacam. Topography and simulated keratometry were assessed using the Atlas corneal topography system (Carl Zeiss Meditec AG, Jena, Germany). Dynamic pupillometry was carried out using the Procyon P2000 pupillometer (Haag-Streit, Bern, Switzerland). Wavefront assessment was performed using the WASCA aberrometer (Carl Zeiss Meditec AG). Single-point pachymetry was performed with the Corneo-Gage Plus (50 MHz) handheld ultrasound pachymeter (Sonogage, Cleveland, OH, USA) by determining the minimum of 10 consecutive central total corneal measurements.

The KC diagnostic criteria included clinical indications such as microscopic signs at the slit-lamp, corneal topographic changes, high refractive astigmatism, reduced CDVA and contrast sensitivity, and significant level of higher-order aberrations, in particular coma. The population included eyes at different stages of the disease, ranging from cases with indisputable KC by topography, but without microscopic signs at the slit-lamp, to advanced cases demonstrating clear microscopic signs such as Vogt striae and substantial corneal thinning. Patients with pellucid marginal degeneration and eyes with pathology other than ectatic degeneration (e.g., corneal scarring) or hydrops were excluded.

Artemis scans were acquired with the patient in a sitting position with the eye coupled to the ultrasound transducer with a normal saline immersion medium contained in a disposable eye seal. During scanning, the patient gazes at a fixation light and eye position is monitored by an infrared camera. Each scan series comprised 4 scans, or 8 hemi-meridians, spaced radially at 45-degree intervals. Scans, consisting of 128 vectors, covered an arc angle of 70° with a radius of curvature in the focal plane of 8 mm, covering a lateral range of approximately 9 mm in the focal plane. We limited the analysis, however, to the central 7 mm because in a few cases data were of insufficient quality beyond the 7 mm zone. ArtPro software was used to determine epithelial and stromal thickness at each position, interpolate between scan planes, and produce 10 × 10 mm Cartesian maps representing layer thickness at 0.1 mm intervals.

The epithelial and stromal thickness maps were processed using MATLAB version 7.11 (The MathWorks Inc., Natick, MA, USA) as previously described (4). In brief, the central 7-mm diameter zone was analyzed to generate features including values and locations of minimum and maximum corneal, epithelial, and stromal thickness and automatic detection of the epithelial pattern that Reinstein et al (3) described as characteristic of KC, i.e., with central thinning surrounded by an annulus of thickened epithelium. The gradients (rate of change of thickness/mm) of epithelial and stromal thicknesses at a series of standard positions were calculated. A total of 126 variables were extracted.

Pentacam scans consisted of 25 images acquired in approximately 2 seconds. An 8-mm diameter best-fit sphere was used in the analysis. The Belin/Ambrósio Enhanced Ectasia display provided by Pentacam is a comprehensive representation of the tomographic structure of the cornea through a combination of elevation and pachymetric data (8-11). Deviation of normality values are implemented for the front (df) and back (db) elevations, thinnest value, pachymetric distribution (dp), and vertical displacement of the thinnest point in relation to the apex (dy). The d values are calculated so that a value of zero represents the average of the normal population and 1 represents the value one standard deviation towards the disease (ectasia) value. A final D is calculated based on a regression analysis that differently weights each parameter.

A total of 114 variables characterizing the front and back surfaces, corneal pachymetry, and Belin/Ambrósio Enhanced Ectasia display (BAD) KC risk indices were exported from the Pentacam. The BAD-D total deviation value KC risk index was separately evaluated as a classifier.

Statistical analyses were performed with IBM (Armonk, NY, USA) SPSS Statistics, version 22. Stepwise linear discriminant analysis (LDA) was used to produce multivariate models utilizing Artemis data alone, Pentacam data alone, and combined Artemis and Pentacam data. The analysis was performed with criteria for variable entry of $p<0.001$ and for variable removal of $p>0.002$. Because covariance was significantly different between normal and KC eyes ($p<0.001$), classification was performed using separate group covariance matrices. *A priori* probabilities were set equal for both groups. Receiver operating characteristic analysis was performed and area under the curve (AUC) determined. Cross-validation, which provides an estimate of how well the classifiers might be expected to perform with new, unknown cases, was performed by repeated random subsampling, using 90% of randomly selected cases as a training set and the remaining 10% as a test set. This was repeated 25 times, using identical random subsets for testing each model.

Results

Table I provides a clinical description of the corneas included in this study, including keratoconus severity score (KSS) (12). A total of 90% of the KC subjects had a KSS of 3, which is characterized by mild disease with possible slit-lamp signs but no corneal scarring and average corneal power ≤52.00 D or higher-order root mean square error between 1.50 and 3.50.

Images derived from Artemis and Pentacam can be qualitatively evaluated by side-by-side comparison or by merger,

TABLE I - Cornea characteristics of normal and keratoconus groups

	Sph, D	Cyl, D	SEQ, D	CDVA, logMAR	Steep K, D	Flat K, D	Mean K, D	CCT, µm	MinCT, µm
Normal									
Mean	-4.12	-1.14	-4.69	-0.035	44.51	43.39	43.95	521.0	516.7
SD	4.58	1.03	4.49	0.086	1.68	1.56	1.57	34.4	34.5
Min	-15.25	-5.50	-16.63	-0.200	40.34	39.40	40.25	445	436
Max	6.75	0.00	5.25	0.200	48.87	47.00	47.94	591	590
Keratoconus									
Mean	-2.01	-3.37	-3.69	0.177	48.79	45.16	46.98	473.1	450.9
SD	4.12	2.90	4.03	0.226	6.05	4.57	5.04	45.9	54.8
Min	-11.50	-12.50	-14.38	0.000	41.00	39.50	40.25	378	297
Max	4.50	0.00	0.25	1.000	66.60	64.70	65.65	549	540

KSS	Normal	KC
0	107	0
1	4	0
2	0	0
3	0	27
4	0	2
5	0	1
N	111	30

CCT = central corneal thickness; CDVA = corrected distance visual acuity; Cyl = cylinder; KC = keratoconus; KSS = keratoconus severity score; MinCT = minimum corneal thickness; SEQ = spherical equivalent; Sph = sphere.

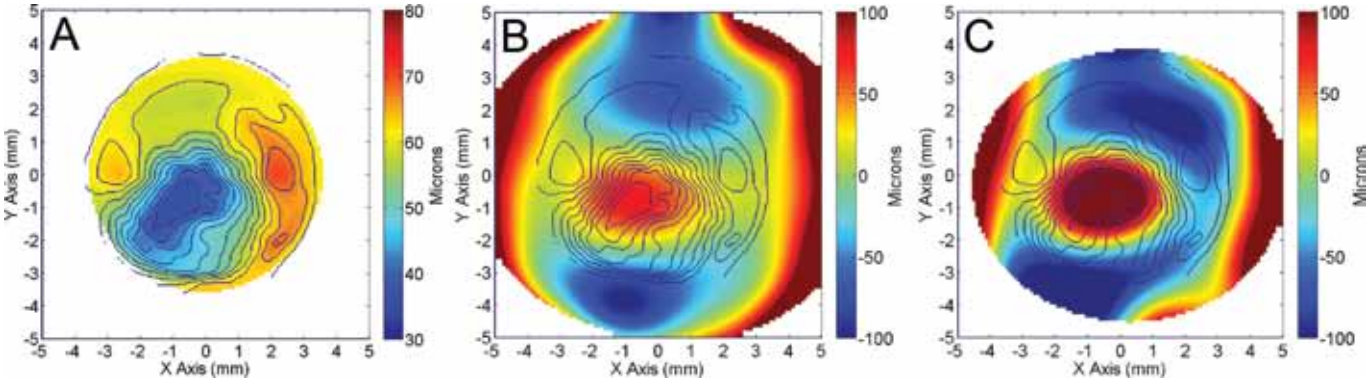

Fig. 1 - Artemis epithelial thickness map (**A**) and Pentacam anterior (**B**) and posterior (**C**) surface elevation maps (difference from 5-mm radius best-fit sphere) of a keratoconic cornea. The epithelial map represents thickness in both color and contour lines. Superimposition of the epithelial contour lines onto the elevation maps reveals that epithelial thinning coincides spatially with hot-spot areas of high elevation (ectasia) of both the anterior and posterior surfaces. Horizontal axis is from temporal (T) to nasal (N).

as illustrated in Figure 1. Superimposition of the epithelial thickness distribution over the anterior or posterior elevation maps, in particular, allows assessment of spatial coincidence between regions of epithelial thinning and positive elevation (ectasia) that would be supportive of a diagnosis of KC.

Statistical analysis, however, allows objective assessment of the capacity of Artemis and Pentacam data to separately or jointly distinguish normal from KC corneas.

Univariate analysis of variance showed 105 of 126 Artemis variables to bear a statistically significant difference ($p<0.05$) between normal and KC eyes. The LDA of the Artemis data resulted in a 4-variable model with a canonical correlation coefficient, R, of 0.860 ($p<0.001$). Table II lists these variables and results of univariate 2-tailed *t* tests comparing means between normal and KC eyes. Also included are the standardized discriminant function coefficients, which are indicative of the relative importance of each variable in the classifier.

Univariate analysis of variance showed 96 of 114 Pentacam variables to bear a statistically significant difference ($p<0.05$) between normal and KC eyes. The LDA of Pentacam data produced a 5-variable model with an R value of 0.857

TABLE II - Artemis variables selected into stepwise multivariate models and their univariate means, standard deviations (SD), and Student t values in separating normal and keratoconus (KC) subjects plus the standardized canonical discriminant function coefficient (Coeff) for each variable in the multivariate model

Variable	Normal, mean (SD)	KC, mean (SD)	t	p value	Coeff
Vertical position of point of minimum corneal thickness, mm	-0.110 (0.339)	-0.680 (0.483)	6.06	<0.001	0.489
Vertical position of point of minimum epithelial thickness, mm	1.535 (1.111)	-0.253 (0.916)	9.05	<0.001	0.398
Minimum stromal thickness, µm	462.1 (34.9)	404.2 (55.1)	5.48	<0.001	0.335
Epithelial thickness gradient about point of minimum corneal thickness, µm/mm	0.625 (0.713)	5.196 (3.024)	-8.22	<0.001	-0.730

Coefficients indicate the relative importance of variables in the overall classification function.

TABLE III - Pentacam variables selected into stepwise multivariate models and their univariate means and standard deviations (SD) in normal and keratoconus (KC) subjects plus the standardized canonical discriminant function coefficient of each variable (Coeff)

Variable	Normal, mean (SD)	KC, mean (SD)	t	p value	Coeff
Deviation of Ambrósio relational thickness, maximum	0.262 (0.755)	2.382 (0.847)	-13.3	<0.001	0.607
Vertical position of point of minimum corneal thickness, mm	-0.241 (0.256)	-0.574 (0.314)	6.00	<0.001	-0.441
Index of vertical asymmetry, mm	0.132 (0.075)	0.809 (0.523)	-7.07	<0.001	0.402
Index of height asymmetry, µm	3.930 (2.994)	18.837 (15.716)	-5.17	<0.001	0.378

(p<0.001). Table III lists these variables, their univariate statistics, and standardized discriminant function coefficients.

The BAD-D values in normal corneas ranged from -0.67 to 1.92 while KC values ranged from 1.87 to 28.54, i.e., there was a small overlap in the distributions. Classification by BAD-D value alone produced a model with an R value of 0.696 (p<0.001). Four KC cases were misclassified, but all normal cases were classified correctly. The ROC AUC, however, was 99.2%, indicating that the missed cases had borderline values, and visual inspection of the complete Belin/Ambrósio display taking all of the analysis presented into account would likely have resulted in a KC diagnosis. Using the BAD-D cutoff of 1.45 suggested by Ambrósio et al (11), all cases of KC would have been correctly classified, but 18 of 111 normal cases would have been classified as KC suspect. A recent article by Ruiseñor Vázquez et al (13) reported optimal BAD-D thresholds of 1.61 and 2.17 for distinguishing normal from subclinical and clinical KC, respectively. Using a threshold of 1.61, all of our KC cases would be correctly classified, but 8 normal cases misclassified as KC. At a threshold of 2.17, no normal cases would have been misclassified, but 3 KC cases would have been missed.

The LDA of the combined Artemis and Pentacam data resulted in a 7-variable model consisting of 3 Artemis variables and 4 Pentacam variables, whose univariate statistics and standardized discriminant function coefficients are shown in Table IV. The R value of the model was 0.910 (p<0.001).

Comparison of the R values of the individual models to that of the combined model shows the increase from 0.86 to 0.91 to be statistically significant (Fisher Z = 1.87, p = 0.031, one-tailed).

The results of all multivariate LDA analyses are summarized in Table V and presented graphically in Figure 2. With all cases included in the training set, all models performed well, with the Artemis misclassifying 1 normal case, the Pentacam missing 2 normal cases and 1 KC, and the combined model missing 1 KC. The AUC values, all near 100%, were not statistically different. The comparative histograms presented in Figure 2 show the combined model to produce the cleanest separation of normal from KC cases compared to either instrument alone or BAD-D alone.

In cross-validation testing, 252 normal and 74 KC corneas randomly excluded from the training sets were presented in total over 25 trials. In cross-validation, the Artemis model misclassified 2 normal and 0 KC corneas, the Pentacam model misclassified 5 normal and 2 KC corneas, and the combined model misclassified 0 normal and 2 KC corneas.

Discussion

Our findings show that both Artemis-based layered pachymetry and Pentacam-derived tomography and topography parameters allowed generation of multivariate models that separated normal corneas from clinical KC. Stepwise LDA

TABLE IV - Variables selected into stepwise multivariate model from combined Pentacam and Artemis data and their univariate means and standard deviations (SD) in normal and keratoconus (KC) subjects plus the standardized canonical discriminant function coefficient of each variable (Coeff)

Variable	Normal, mean (SD)	KC, mean (SD)	t	p Value	Coeff
Deviation of Ambrósio relational thickness, maximum	0.262 (0.755)	2.382 (0.847)	-13.3	<0.001	0.438
Vertical position of point of minimum corneal thickness, mm	-0.241 (0.256)	-0.574 (0.314)	6.00	<0.001	-0.462
Index of vertical asymmetry, mm	0.132 (0.075)	0.809 (0.523)	-7.07	<0.001	0.898
Index of height decentration, µm	0.0073 (0.0065)	0.0675 (0.0592)	-5.56	<0.001	-0.637
Epithelial thickness gradient about point of minimum corneal thickness, µm/mm	0.625 (0.713)	5.196 (3.024)	-8.22	<0.001	1.512
Epithelial thickness gradient superiorly about point of minimum corneal thickness, µm/mm	-0.091 (1.027)	4.385 (3.329)	-7.27	<0.001	-1.078
Vertical position of point of minimum epithelial thickness, mm	1.535 (1.111)	-0.253 (0.916)	9.05	<0.001	-0.393

TABLE V - Summary of sensitivity and specificity of each linear discriminant model, and the area under the receiver operating characteristic curve (AUC) for the discriminant function

Model	Classification (training set), %			Cross-validation, %	
	Sensitivity	Specificity	AUC	Sensitivity	Specificity
Artemis	100.0	99.1	100.00	100.0	99.2
Pentacam	96.7	98.2	99.72	97.3	98.0
Combined	96.7	100.0	99.97	97.3	100.0

An AUC of 100% indicates complete separation of groups at some optimal discriminant function threshold value. Cross-validation results were based on classification performance on random sets of 10% of cases excluded from the training set in 25 consecutive trials.

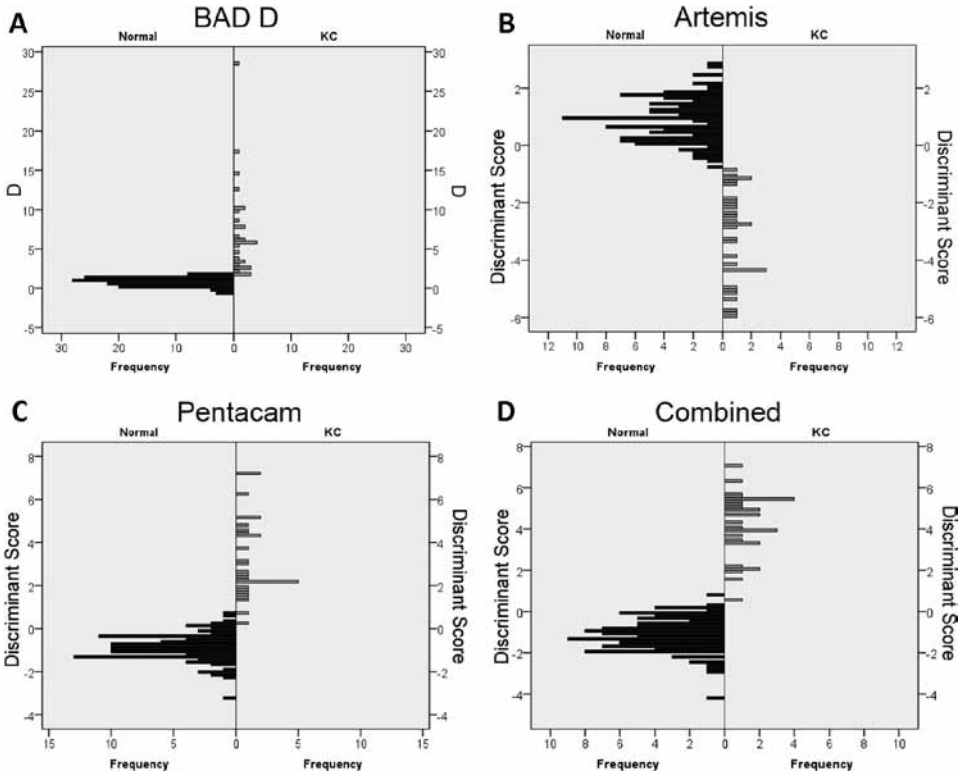

Fig. 2 - Comparative histograms demonstrating the distribution of classifier values for normal and KC cases for models based on (**A**) Belin/Ambrósio Enhanced Ectasia display D (BAD-D), (**B**). Artemis, (**C**) Pentacam and (**D**) combined Artemis plus Pentacam.

of combined Artemis and Pentacam data resulted in a model that included variables from both devices. The two most heavily weighted variables were derived from the Artemis and related to the epithelial thickness gradient (the spatial rate of epithelial thickness change, µm/mm) near the cone apex. Since the stepwise variable selection procedure tends to exclude correlated variables and to choose a minimal set of statistically independent variables to achieve separation of groups, the result indicates that at least for differentiation of normal (myopic) corneas from clinical KC, each technique contributes independent diagnostic information. Indeed, all Artemis variables included in the combined model related to the epithelial thickness distribution, while Pentacam variables related to corneal thickness distribution and topography. In cross-validation, the Artemis-alone and combined models had comparable performance (2 misclassifications each), both somewhat better than the Pentacam-alone model. Statistically, the combined model, with an R^2 (which represents the fraction of variation explained by the model) of 0.83, was superior to Artemis or Pentacam alone, both of which had R^2 of approximately 0.73.

In the present study, parameters separately derived from each instrument were combined, but it would be advantageous to coregister Pentacam and Artemis maps and to compare features from each device at each position with those of maps representing the normative database so that regions deviating from the norm are highlighted.

In this report, we limited subjects solely to patients who were clearly normal or KC based on independent clinical criteria to avoid ambiguity in interpretation of results. We recently demonstrated the effectiveness of algorithms based on epithelial thickness distribution in identification of KC in clinically and topographically normal-appearing fellow eyes of subjects with unilateral KC, with 5 of 10 fellow eyes identified as KC (14). While our present findings demonstrate the higher statistical power of the combined model, application of the classifier to larger numbers of preclinical and forme fruste KC unambiguously diagnosed as KC by evidence of progression or in unilateral KC will be required to demonstrate the effectiveness of the methods developed in this study for screening, and these studies are underway.

Disclosures

Financial support: Supported in part by NIH grant EY019055 and an unrestricted grant to the Department of Ophthalmology of Columbia University from Research to Prevent Blindness.
Conflict of interest: Drs. Silverman and Reinstein have a proprietary interest in the Artemis technology (ArcScan, Inc., Morrison, CO, USA) and are the authors of relevant patents administered by the Cornell Center for Technology Enterprise and Commercialization, Ithaca, NY, USA. The remaining authors have no proprietary or financial interest in the materials presented herein.

References

1. Reinstein DZ, Silverman RH, Sutton HF, Coleman DJ. Very high-frequency ultrasound corneal analysis identifies anatomic correlates of optical complications of lamellar refractive surgery: anatomic diagnosis in lamellar surgery. Ophthalmology. 1999;106(3):474-482.
2. Reinstein DZ, Gobbe M, Archer TJ, Silverman RH, Coleman DJ. Epithelial, stromal, and total corneal thickness in keratoconus: three-dimensional display with artemis very-high frequency digital ultrasound. J Refract Surg. 2010;26(4):259-271.
3. Reinstein DZ, Archer TJ, Gobbe M. Corneal epithelial thickness profile in the diagnosis of keratoconus. J Refract Surg. 2009;25(7):604-610.
4. Silverman RH, Urs R, Roychoudhury A, Archer TJ, Gobbe M, Reinstein DZ. Epithelial remodeling as basis for machine-based identification of keratoconus. Invest Ophthalmol Vis Sci. 2014;55(3):1580-1587.
5. Li Y, Tan O, Brass R, Weiss JL, Huang D. Corneal epithelial thickness mapping by Fourier-domain optical coherence tomography in normal and keratoconic eyes. Ophthalmology. 2012;119(12):2425-2433.
6. Rocha KM, Perez-Straziota CE, Stulting RD, Randleman JB. SD-OCT analysis of regional epithelial thickness profiles in keratoconus, postoperative corneal ectasia, and normal eyes [erratum 2013;29:234]. J Refract Surg. 2013;29(3):173-179.
7. Qin B, Chen S, Brass R, et al. Keratoconus diagnosis with optical coherence tomography–based pachymetric scoring system. J Cataract Refract Surg. 2013;39(12):1864-1871.
8. Ambrósio R Jr, Alonso RS, Luz A, Coca Velarde LG. Corneal-thickness spatial profile and corneal-volume distribution: tomographic indices to detect keratoconus. J Cataract Refract Surg. 2006;32(11):1851-1859.
9. Ambrósio R Jr, Caiado AL, Guerra FP, et al. Novel pachymetric parameters based on corneal tomography for diagnosing keratoconus. J Refract Surg. 2011;27(10):753-758.
10. Ambrósio R Jr, Nogueira LP, Caldas DL, et al. Evaluation of corneal shape and biomechanics before LASIK. Int Ophthalmol Clin. 2011;51(2):11-38.
11. Ambrósio R Jr, Faria-Correia F, Ramos I, et al. Enhanced screening for ectasia susceptibility among refractive candidates: the role of corneal tomography and biomechanics. Curr Ophthalmol Rep. 2013;1:28-38.
12. McMahon TT, Szczotka-Flynn L, Barr JT, et al; CLEK Study Group. A new method for grading the severity of keratoconus: the Keratoconus Severity Score (KSS). Cornea. 2006;25(7):794-800.
13. Ruiseñor Vázquez PR, Galletti JD, Minguez N, et al. Pentacam Scheimpflug tomography findings in topographically normal patients and subclinical keratoconus cases. Am J Ophthalmol. 2014;158(1):32-40.e2.
14. Reinstein DZ, Archer TJ, Urs R, Gobbe M. RoyChoudhury A, Silverman RH. Detection of keratoconus in the clinically and algorithmically topographically normal fellow-eyes of unilateral keratoconus using epithelial thickness analysis. J Refract Surg. 2015;31(11):736-744.